

Modeling suspended sediment sources and transport in the Ishikari River basin, Japan using SPARROW

Weili Duan^{1,2}, Bin He¹, Kaoru Takara³, Pingping Luo³, Daniel Nover⁴ and Maochuan Hu²

¹State Key Laboratory of Lake Science and Environment, Nanjing Institute of Geography and Limnology, Chinese Academy of Sciences, Nanjing 210008, China

²Department of Civil and Earth Resources Engineering, Graduate School of Engineering, Kyoto University, Kyoto, Japan

³Disaster Prevention Research Institute, Kyoto University, Kyoto, Japan

⁴AAAS Science and Technology Policy Fellow, U.S. Environmental Protection Agency, Global Change Research Group, Washington, DC, 20010, USA

ABSTRACT: It is important to understand the mechanisms that control the fate and transport of suspended sediment (SS) in rivers, because high suspended sediment loads have significant impacts on riverine hydroecology. In this study, the watershed model SPARROW (SPAtially Referenced Regression on Watershed Attributes) was applied to estimate the sources and transport of SS in surface waters of the Ishikari River basin (14 330 km²), the largest watershed on Hokkaido Island, Japan. The final developed SPARROW model has four source variables (developing lands, forest lands, agricultural lands, and stream channels), three landscape delivery variables (slope, soil permeability, and precipitation), two in-stream loss coefficients including small stream (streams with drainage area < 200 km²), large stream, and reservoir attenuation. The model was calibrated using measurements of SS from 31 monitoring sites of mixed spatial data on topography, soils and stream hydrography. Calibration results explain approximately 95.96% (R²) of the spatial variability in the natural logarithm mean annual SS flux (kg yr⁻¹) and display relatively small prediction errors at the 31 monitoring stations. Results show that developing-land is associated with the largest sediment yield at around 1-006.27 kg km⁻² yr⁻¹, followed by agricultural-land (234.21 kg

Comment [MM1]: These numbers should be rounded to significant digits: e.g. 1010 kg km-2 yr-1 and 235 kg km-2 yr-1.

Formatted: Highlight

Formatted: Highlight

24 | $\text{km}^{-2} \text{ yr}^{-1}$). Estimation of incremental yields shows that 35.11% comes from agricultural lands,
25 | 23.42% from forested lands, 22.91% from developing lands, and 18.56% from stream channels. The
26 | results of this study improve our understanding of sediments production and transportation in the
27 | Ishikari River basin in general, which will benefit both the scientific and the management
28 | community in safeguarding water resources.

29 | **Key Words:** sediment, Ishikari River basin, SPARROW, transportation, land use

30 | 1 Introduction

31 | Suspended sediment (SS) is ubiquitous in aquatic ecosystems and contributes to bottom
32 | material composition, water-column turbidity, and chemical constituent transport. However,
33 | sediment is the largest water pollutant by volume and excessive sediment can have dramatic
34 | impacts on both water quality and aquatic biota (Bilotta and Brazier, 2008). High turbidity can
35 | significantly reduce or limit light penetration into water with implications for primary production
36 | and for populations of fish and aquatic plants. In addition, excessive sedimentation can bring more
37 | pollutants containing organic matter, animal or industrial wastes, nutrients, and toxic chemicals
38 | because sediment comes mainly from forestlands, agricultural fields, highway runoff, construction
39 | sites, and mining operations (Le et al., 2010; Srinivasa et al., 2010), which always cause water
40 | quality deterioration and therefore is a common and growing problem in rivers, lakes and coastal
41 | estuaries (Dedkov and Mozzherin, 1992; Ishida et al., 2010; Meade et al., 1985). Eutrophication due
42 | to nutrient pollution, for example, is a widespread sediment-related problem recognized at sites
43 | world-wide (Conley et al., 2009). Also, in the U.S., approximately 25% of stream length (167,092
44 | miles) has been negatively impacted by excessive sediment loads (U. S. Environmental Protection
45 | Agency [USEPA](#), 2006).

Comment [MM2]: These values in % should be rounded maybe even to full percentage, i.e.: 35%, 23%, 23 %, and 19%. I don't believe that the model is that "precise" in these estimations.

Formatted: Highlight

Formatted: Highlight

Formatted: Highlight

Formatted: Highlight

46 Similarly, sediment accumulation can reduce the transport capacity of roadsides ditches,
47 streams, rivers, and navigation channels and the storage capabilities of reservoirs and lakes, which
48 cause more frequent flooding. For example, dams will gradually lose their water storage capacity as
49 sediment accumulates behind the dam (Fang et al., 2011); Erosion of river banks and increased
50 sedimentation are also impacting the Johnstone River catchment (Hunter and Walton, 2008) and the
51 estuary in the Tuross River catchment of coastal southeast Australia (Drewry et al., 2009) in
52 clogging of land and road drainage systems and river systems. Therefore, as SS are fundamental to
53 aquatic environments and impairments due to enhanced sediment loads are increasingly damaging
54 water quality and water resources infrastructure, it is extremely important to develop both
55 monitoring systems and technologies to track and to reduce the volume of SS in order to safeguard
56 freshwater systems.

57 Sediment sources can be separated into sediment originating in upland regions, sediment
58 from urban areas, and sediment eroded from channel corridors (Langland ~~and Croninet al.~~, 2003).
59 Land use impacts are commonly seen as resulting in increased sediment loads and therefore as an
60 inadvertent consequence of human activity. Moreover, land use and land use change are also
61 important factors influencing erosion and sediment yields. For example, urbanization may
62 ultimately result in decreased local surface erosion rates when large areas are covered with
63 impervious surfaces such as roadways, rooftops, and parking lots (Wolman, 1967); because of the
64 increased exposure of the soil surface to erosive forces as a result of the removal of the native
65 vegetative cover, agricultural lands can drastically accelerate erosion rates (Lal, 2001). In addition,
66 stream channel erosion can be a major source of sediment yield from urbanizing areas (Trimble,
67 1997).

68 In the Japanese context, high suspended sediment loads is increasingly recognized as an
69 important problem for watershed management (Mizugaki et al., 2008; Somura et al., 2012). For
70 example, the Ishikari River basin has long been plagued by high suspended sediment loads,

71 generally causing high turbidity along the river, including in Sapporo, Hokkaido's economic and
72 government center. The pervasiveness of the problem has generated several sediment management
73 studies in the Ishikari River basin. Asahi et al. (2003) found that it is necessary to consider tributary
74 effects directly and that sediment discharged from tributaries contributes to the output sediment
75 discharged from the river's mouth. Wongsu and Shimizu (2004) indicated land-use change has a
76 significant effect on soil eroded from hill slopes, but no significant effect on flooding for Ishikari
77 basin. Ahn et al. (2009) concluded that sedimentation rate increased in the Ishikari River floodplain
78 because of agricultural development on the floodplains. However, detailed accounting of sediment
79 sources (e.g. the type of land-use) and transport in the Ishikari River basin remains poorly
80 understood.

81 Computer based modeling is an essential exercise both for organizing and understanding
82 the complex data associated with water quality conditions and for development of management
83 strategies and decision support tools for water resource managers (Somura et al., 2012). Recent
84 applications of the GIS-based watershed model SPATIALLY Referenced Regression On Watershed
85 attributes (SPARROW) (Smith et al., 1997) in the United States have advanced understanding of
86 nutrient sources and transport in large regions such as the Mississippi River Basin (Alexander et al.,
87 2000; 2007) and smaller watersheds such as the Chesapeake Bay watershed (Langland et al., 2010)
88 and those draining to the North Carolina coast (McMahon et al., 2003).

Comment [MM3]: This reference is not listed at the end in the list of references.

89 In this study, we use the SPARROW principle and framework to develop a regional-scale
90 sediment transport model for the Ishikari River basin in Hokkaido, Japan. The concrete objectives
91 are (1) to calibrate SS SPARROW for Ishikari River basin on the basis of 31 stations; (2) to use the
92 calibrated model to estimate mean annual SS conditions; and (3) to quantify the relative
93 contribution of different SS sources to instream SS loads. These efforts are undertaken with the
94 ultimate goal of providing the information of total and incremental sediments loads in different
95 sub-basin that will help resource managers identify priority sources of pollution and mitigate this

96 pollution in order to safeguard water resources and protect aquatic ecosystems.

97 **2 Materials and methods**

98 **2.1 Study area**

99 The Ishikari River, the third longest river in Japan (Fig. 1), originates from Mt.
100 Ishikaridake (elevation 1967 m) in the Taisetsu Mountains of central Hokkaido, passes through the
101 west of Hokkaido, and flows into the Sea of Japan, with a total sediment discharge of around 14.8
102 cubic kilometres per year. The river has the largest river basin with total drainage area of 14 330
103 km², the north-south and east-west distance of which is about 170 and 200 km, respectively. The
104 Ishikari plain occupies most of the basin's area, which is surrounded by rolling hills and is the
105 lowest land in Japan (the highest elevation is less than 50 m) and consequently the best farming
106 region in the country. The Ishikari River basin has cold snowy winters and warm, non-humid
107 summers. Sediment load is very low in the cold winter except for the temporary snowmelt at
108 positive degree air temperature and high in the snowmelt season of mid-March to May and heavy
109 rainfalls in May- late November. In this basin, the regional average August temperature ranges from
110 17 to 22 °C, while the average January temperature ranges from −12 to −4 °C; the regional annual
111 precipitation was 850-1300 mm from 1980 to 2011.

112 **2.2 Modeling tools**

113 Based on the mechanistic mass transport components including surface-water flow paths
114 (channel time of travel, reservoirs), non-conservative transport processes (i.e., first-order in-stream
115 and reservoir decay), and mass-balance constraints on model inputs (sources), losses (terrestrial and
116 aquatic losses/storage), and outputs (riverine nutrient export), the SPARROW modeling approach
117 performs a nonlinear least-squares multiple regression to describe the relation between spatially
118 referenced watershed and channel characteristics (predictors) and in-stream load (response)

(Schwarz et al., 2006). This allows nutrient supply and attenuation to be tracked during water transport through streams and reservoirs and assesses the natural processes that attenuate constituents as they are transported from land and upstream (Preston et al., 2009). Figure 2 gives a graphical description of the SPARROW model components. Monitoring station flux estimation refers to the estimates of long-term flux used as the response variable in the model. Flux estimates at monitoring stations are derived from station-specific models that relate contaminant concentrations from individual water-quality samples to continuous records of streamflow time series. To obtain reliable unbiased estimates, the Maintenance of Variance-Extension type 3 (MOVE. 3) and the regression model Load Estimator (LOADEST) were applied to develop regression equations and to estimate monitoring station flux (for calculation details see Duan et al., 2013).

For the model-estimated flux, the SPARROW modeling can generally be defined by the following equation (Alexander et al., 2007):

$$F_i^* = \left[\left(\sum_{j \in J(i)} F_j' \right) A(Z_i^S, Z_i^R; \theta_S, \theta_R) + \left(\sum_{n=1}^{N_S} S_{n,i} \alpha_n D_n(Z_i^D; \theta_D) \right) A'(Z_i^S, Z_i^R; \theta_S, \theta_R) \right] \varepsilon_i \quad (1)$$

where F_i^* is the model-estimated flux for contaminant leaving reach i . The first summation term represents the sediment flux that leaves upstream reaches and is delivered downstream to reach i , where F_j' denotes measured sediment flux (F_j^M) when upstream reach j is monitored and equals the given model-estimated flux (F_j^*) when it is not. $A(\cdot)$ is the stream delivery function representing sediment loss processes acting on flux as it travels along the reach pathway, which defines the fraction of sediment flux entering reach i at the upstream node that is delivered to the reach's downstream node. Z^S and Z^R represent the function of measured stream and reservoir characteristics, respectively, and θ_S and θ_R are their corresponding coefficient vectors. Here, stream reach and watershed characteristics such as stream length, direction of water flow, connectivity, mean annual streamflow, water traveltime per unit length, reservoir characteristics like

143 surface area, and local and total drainage area were present in the digital stream network dataset and
 144 reflect parameters required by the model. The second summation term denotes the amount of
 145 sediment flux introduced to the stream network at reach i , which is composed of the flux originating
 146 from specific sediment sources, indexed by $n = 1, 2, \dots, N_S$. Each source has a source variable,
 147 denoted S_n , and its corresponding source-specific coefficient, α_n . This coefficient retains the units
 148 that convert the source variable units to flux units. The function $D_n(\cdot)$ represents the land-to-water
 149 delivery factor. The land-to-water delivery factor is a source-specific function of a vector of
 150 delivery variables, denoted by Z_i^θ , and an associated vector of coefficients θ_D . The function $A'(\cdot)$
 151 represents the fraction of flux originating in and delivered to reach i that is transported to the
 152 reach's downstream node and is similar in form to the stream delivery factor defined in the first
 153 summation term of the equation. If reach i is classified as a stream (as opposed to a reservoir
 154 reach), the sediment introduced to the reach from its incremental drainage area receives the square
 155 root of the reach's full in-stream delivery. This assumption is consistent with the notion that
 156 contaminants are introduced to the reach network at the midpoint of reach i and thus are subjected
 157 to only half of the reach's time of travel. Alternatively, for reaches classified as reservoirs, we
 158 assume that the sediment mass receives the full attenuation defined for the reach. The multiplicative
 159 error term in Equation (1), ε_i , is applicable in cases where reach i is a monitored reach; the error
 160 is assumed to be independent and identically distributed across independent sub-basin in the
 161 intervening drainage between stream monitoring stations. This item can also be used for
 162 unmonitored reaches.

163 The reach-loss and reservoir-loss are used as the mediating factors affecting the
 164 mobilization of sediment from the stream network. Reach-loss variable is nonzero only for stream
 165 reaches, and is defined for two separate classes, shallow-flowing (small) streams versus
 166 deep-flowing (large) streams. Since stream depth is not known, streams with drainage area < 200
 167 km^2 are classified as shallow, small streams. The reservoir-loss is denoted by areal hydraulic load of

the reservoir, which is computed as the quotient of mean annual impoundment outflow and surface area (Hoos and McMahon, 2009). Sediment loss in streams is modeled according to a first-order decay process (Chapra, 1997; Brakebill, et al., 2010) in which the fraction of the sediment mass originating from the upstream node and transported along reach i to its downstream node is estimated as a continuous function of the mean water time of travel (T_i^S ; units of time) and mean water depth, D_i , in reach i , such that

$$A(Z_i^S, Z_i^R; \theta_S, \theta_R) = \exp\left(-\theta_S \frac{T_i^S}{D_i}\right) \quad (2)$$

where θ_S is an estimated mass-transfer flux-rate coefficient in units of length time⁻¹. The rate coefficient is independent of the properties of the water volume that are proportional to water volume, such as streamflow and depth (3). The rate can be re-expressed as a reaction rate coefficient (time⁻¹) that is dependent on water-column depth by dividing by the mean water depth.

Sediment loss in lakes and reservoirs is modeled according to a first-order process (Chapra, 1997; Brakebill, et al., 2010) in which the fraction of the sediment mass originating from the upstream reach node and transported through the reservoir segment of reach i to its downstream node is estimated as a function of the reciprocal of the areal hydraulic load $(q_i^R)^{-1}$ (units of time length⁻¹) for the reservoir associated with reach i and an apparent settling velocity coefficient (θ_R ; units of length time⁻¹), such that

$$A(Z_i^S, Z_i^R; \theta_S, \theta_R) = \frac{1}{1 + \theta_R (q_i^R)^{-1}} \quad (3)$$

The areal hydraulic load is estimated as the quotient of the outflow discharge to the surface area of the impoundment.

188 **2.3 Input data**

189 In this study, input data for building SPARROW models is classified into (Table 1): 1)
190 stream network data to define stream reaches and catchments of the study area; 2) loading data for
191 many monitoring stations within the model boundaries (dependent variables); 3) sediment sources
192 data describing all of the sources of the sediment being modeled (independent variables); and 4)
193 data describing the environmental setting of the area being modeled that causes statistically
194 significant variability in the land- to- water delivery of sediment (independent variables). Input data
195 types are described in more detail below.

196 **2.3.1 The stream network**

197 The hydrologic network used for the SPARROW model of the Ishikari River basin is
198 derived from a 50 m digital elevation model (DEM) (Fig. 1), which has 900 stream reaches, each
199 with an associated sub-basin. The stream network mainly contains stream reach and sub-basin
200 characteristics such as stream length, direction of water flow, reservoir characteristics like surface
201 area, and local and total drainage area. For example, the areas of sub-basin range from 0.009 to 117
202 km² with a median of 15.9 km². However, mean water flow is not reported for each stream reach,
203 suggesting that we cannot calculate the SS concentration at the stream reach scale but can calculate
204 the total yield SS for each associated sub-basin.

205 **2.3.2 Stream load data**

206 Suspended sediment concentration and daily flow data are collected to calculate the
207 long-term (from 1985 to 2010) mean SS flux at every monitoring station. Thirty-one monitoring
208 stations were chosen for model calibration in this study (Fig. 1). SS concentration and daily flow
209 data were collected at each site for the period from 1985 to 2010 by the National Land with Water
210 Information (<http://www1.river.go.jp/>) monitoring network (Fig. 3). However, some streamflow

gaging stations have short periods of record or missing flow values but do not over 10% of the time periods. A streamflow record extension method called the Maintenance of Variance-Extension type 3 (MOVE.3) (Vogel and Stedinger, 1985) is employed to estimate missing flow values or to extend the record at a short-record station on the basis of daily streamflow values recorded at nearby, hydrologically similar index stations. On this basis, the FORTRAN Load Estimator (LOADEST), which uses time-series streamflow data and constituent concentrations to calibrate a regression model that describes constituent loads in terms of various functions of streamflow and time, is applied to estimate SS loads. The output regression model equations take the following general form (Runkel et al., 2004):

$$\ln(L_i) = a + b\ln Q + c\ln Q^2 + d\sin(2\pi dtime) + e\cos(2\pi dtime) + f dtime + g dtime^2 + \varepsilon \quad (4)$$

where L_i is the calculated load for sample i ; Q is stream discharge; $dtime$ is time, in decimal years from the beginning of the calibration period; ε is error; and a, b, c, d, e, f, g are the fitted parameters in the multiple regression model. The number of parameters may be different at different stations, depending on the lowest Akaike Information Criterion (AIC) values (for details please see Duan et al., 2013).

$$AIC = 2k - 2\ln(L) \quad (5)$$

where k is the number of parameters in the statistical model, and L is the maximized value of the likelihood function for the estimated model.

The mean annual load is normalized to the 2006 base year at the 31 monitoring stations to address the problem of incompatibility in periods of record by using normalizing or detrending methods (for detailed process please see Schwarz et al., 2006).

2.3.3 Sediment source data

SS source variables tested in the Ishikari SPARROW model include estimates of

developing lands, forest lands, agricultural lands, and stream channels. Estimates of land use were developed using data derived from the Policy Bureau of the Ministry of Land, Infrastructure, Transport and Tourism, Japan, 2006, which mainly contains 11 types of land use (see Fig. 4). It was then merged into 4 types: developing land, forest land, agricultural land, and water land. Finally, different lands are allocated to individual sub-basin using GIS zonal processes. Arc Hydro Tools is employed to get reach length which denotes the streambed source.

2.3.4 Environmental setting data

Climatic and landscape characteristics considered candidates for SS-transport predictors include climate, topography and soil (Asselman et al., 2003; Dedkov and Mozzherin, 1992). Here, slope, soil permeability, and precipitation are used to evaluate the influences of “land-to-water” delivery terms. Basin slope is obtained using the GIS surface tool (see Fig.5 (a)). Soil permeability and clay content (see Fig.5 (b)) are estimated using data derived from the 1:5,000,000-scale FAO/UNESCO Soil Map of the World (FAO-[UNESCO-ISRIC](#), 1988) and the National and Regional Planning Bureau, Japan. Mean annual precipitation data, representing the 20-year (1990-2010) average, were obtained from daily precipitation data at 161 weather stations (see Fig. S1) in Hokkaido from 1990 to 2010; that is, we first interpolated the mean annual precipitation over Hokkaido using a conventional kriging technique on the basis of 161 stations, and then clipped the mean annual precipitation distribution for the Ishikari River basin. Finally, all these watershed-average values were used to calculate estimates for each sub-basin in the Ishikari model area using the ZONALMEAN and ZONALSTATISTICAL functions (zonal spatial analyst methods) of ArcGIS 10.

2.4 Model calibration and application

Considering the calibration of the SPARROW model requires long-term averaging and load adjustments for changes in flow and sources, the final SPARROW model was statistically

calibrated using estimates of mean annual SS flux at 31 monitoring stations (see Input data). The explanatory variables represented statistically significant or otherwise important geospatial variables, and the measures of statistically significant are based on statistical evaluations of the t statistics (ratio of the coefficient value to its standard error). The t statistics are asymptotically distributed as a standard normal. The statistical significance ($\alpha=0.05$) of the coefficients for each of the SS source terms (which were constrained to be positive) were determined by using a one-sided t-test, and the significance of the coefficients for each of the land- to- water delivery terms (which were allowed to be positive or negative, reflecting either enhanced or attenuated delivery, respectively) and the variables representing SS loss in free-flowing streams and impoundments were determined by using a two-sided t-test (Schwarz et al., 2006). The yield R-squared (R^2), the root mean squared error (RMSE), and the residuals for spatial patterns were the conventional statistical diagnostics used to assess the overall SPARROW model accuracy and performance.

According to the equations of SPARROW, the calibrated model can be used to identify the largest local SS sources; that is, the sediment source contributing the most to the incremental SS yield for each catchment in Ishikari River basin can be calculated. In addition, the models can be used to estimate the contribution from each sediment source to the total SS loads predicted for each reach. Total loads were the predicted load contributed from all upstream landscape sediment sources. Finally, the factors that affect mean annual transport in the Ishikari River basin can be identified.

3 Results and discussion

3.1 Model calibration

Model calibration results for the log transforms of the summed quantities in Equation (1) and non-linear least-squares estimates are presented in Table 2, which explains approximately

282 95.96% (R^2) of the spatial variation in the natural logarithm of mean annual SS flux (kg yr^{-1}), with a
283 mean square error (MSE) of 0.323 kg yr^{-1} , suggesting that the SS predicted by the model has litter
284 error compared with the observation load.

Comment [MM4]: This is not understandable: litter. Have you meant smaller?

285 The plot of predicted and observed SS flux is shown in Fig._6, demonstrating model
286 accuracy over a wide range of predicted flux and stream sizes. Generally, for a good SPARROW
287 model, the graphed points should exhibit an even spread about the one-to-one line (the straight line
288 in Fig._6) with no outliers. However, a common pattern expressed in Fig._6 for final SPARROW
289 SS model is the tendency for larger scatter among observations with smaller predicted flux- a
290 pattern of heteroscedasticity. One likely cause for this pattern is greater error in the measurement of
291 flux in small sub-basin due to greater variability in flow or to greater relative inhomogeneity of
292 sediment sources within small sub-basin (Schwarz et al., 2006). Appropriate assignment of weights
293 reflecting the relative measurement error in each observation (plus an additional common model
294 error) can improve the coefficient estimates and correct the inference of coefficient error if the
295 heteroscedasticity is caused by measurement error. On the other hand, the observations can be
296 weighted to improve the coefficient estimates and correct their estimates of error if the
297 heteroscedasticity is due to structural features of the SPARROW model. Figure 7 shows the
298 standardized residuals at the 31 monitoring sites. Monitoring sites with over- predictions (< 0)
299 mainly exist in the middle area of the Ishikari River basin, and under- predictions (> 0) exist in the
300 upper and lower areas. The Studentized residual is useful for identifying outliers, and if greater than
301 3.6 are generally is considered an outlier warranting further investigation (Schwarz et al., 2006).
302 Overall, the final model does not show evidence of large prediction biases over the monitoring sites.

303 With the exception of stream channels, all of the source variables modeled are statistically
304 significant (P-value < 0.05), with the estimated coefficient representing an approximate estimate of
305 mean sediment yield for the associated land use (Table 2). The largest intrinsic sediment yield is
306 associated with developing land, the estimated value of which is around $1006.27 \text{ kg km}^{-2} \text{ yr}^{-1}$. Land

Formatted: Highlight

development, including removing cover and developing cuts and fills, can increase potential erosion and sediment hazards on-site by changing water conveyance routes, soil compaction (both planned and unplanned), longer slopes and more and faster stormwater runoff. With the analysis of factors affecting sediment transport from uplands to streams (mean basin slope, reservoirs, physiography, and soil permeability), developing land was also the largest sediment source reported in Brakebill et al. (2010) and Schwarz (2008). Agricultural land has the second highest sediment yield with an estimated value of around 234.21 kg km⁻² yr⁻¹ and forest land has the lowest sediment yield with an estimated value of around 75.55 kg km⁻² yr⁻¹.

Comment [MM5]: You are using the wording "around" and then giving the number with two decimal digits.

Formatted: Highlight

Formatted: Highlight

Land-to-water delivery for sediment land sources is powerfully mediated by watershed slope, soil permeability, and rainfall, all of which are statistically significant (Table 2). As expected, Table 2 shows that sediment produced from land transport to rivers is most efficient in areas with greater basin slope, less permeable soils, and greater rainfall, which is consistent with the results calculated by Brakebill et al. (2010). The alteration of these factors can directly and indirectly cause changes in sediment degradation and deposition, and, finally, to the sediment yield (Luce and Black, 1999; Nelson and Booth, 2002). Increased rainfall amounts and intensities can directly increase surface runoff, leading to greater rates of soil erosion (Nearing et al., 2005; Ran et al., 2012) with consequences for productivity of farmland (Julien and Simons, 1985). Watershed slope and soil permeability have a powerful influence on potential surface runoff as they affect the magnitude and rate of eroded sediment that may be transported to streams (Brakebill et al., 2010).

The coefficient for in-stream loss indicates that sediment is removed from large streams (about 0.000012 day⁻¹) and accumulates in small streams (about -0.044 day⁻¹). These results run contrary to several published examples. For example, Schwarz (2008) argued that greater streamflow causes an increase in the amount of sediment generated from stream channels. The reasons for these results could be the criterion of the two kinds of streams. In this study, streams with drainage area < 200 km² are shallow, small streams, which tend to attenuate the sediments; on

the contrary, streams with drainage area $> 200 \text{ km}^2$ are big streams, which tend to create the sediments. Sediment storage is statistically significant in reservoirs (dams), the estimated value of which is around 26.28 m yr^{-1} . This value is much less than a coefficient of 234.92 m yr^{-1} reported for the Chesapeake Bay Watershed SPARROW model (Brakebill et al., 2010), one possible reason of which maybe is that the reservoirs in the Ishikari River basin have less storage capacity compared with the reservoirs in the Chesapeake Bay. However, the value is similar to 36 m yr^{-1} computed by the conterminous U.S. SPARROW model (Schwarz, 2008).

Formatted: Highlight

Formatted: Highlight

Comment [MM6]: You see, the result is given in m yr^{-1} with no decimal digits.

Formatted: Highlight

3.2 Model application

Because data from sampling stream networks suffer from sparseness of monitoring stations, spatial bias and basin heterogeneity, describing regional distributions and exploring transport mechanism of sediment is one of the challenges of sediment assessment programs. Through the stream network, SPARROW can link in-stream water quality to spatially referenced information on contaminant sources and other watershed attributes relevant to contaminant transport (Smith et al., 1997). After calibration, the SPARROW model of total suspended sediment can be applied to evaluate the stream-corridor sediment supply, storage, and transport properties and processes in a regional context, which can inform a variety of decisions relevant to resource managers. Here, in order to further explore and manage sediment sources, we predict and analyze the spatial distribution of total sediment and incremental sediment yields, and estimate the amount of sediment generated by source is described in each incremental basin.

The total yields (load per area) represent the amount of sediment including upstream load and local catchment load contributed to each stream reach, and the incremental yields represent the amount of sediment generated locally independent of upstream supply, and contributed to each stream reach, normalized by the local catchment area (see Fig. S2) (Ruddy et al., 2006). Figure 8 (a) shows the spatial distribution of the total yields, describing the sediment mass entering streams per

unit area of the incremental drainages of the Ishikari River basin associated with the stream network (Fig. 1). It is mediated by climatic and landscape characteristics and delivered to the Ishikari gulf of the Sea of Japan after accounting for the cumulative effect of aquatic removal processes. Figure 8 (a) shows that total yields, ranging from 0.03 to 1190 kg ha⁻¹ yr⁻¹ (mean=101 kg ha⁻¹yr⁻¹), concentrate in the sub-basin along the middle and lower reaches of the Ishikari River. Like total yields, much of the incremental sediment yields are distributed in similar areas (see Fig.8 (b)), the largest of which is greater than 150 kg ha⁻¹yr⁻¹. These two kinds of predictions provide localized estimates of sediment that are useful in evaluating local contributions of sediment in addition to identifying geographic areas of potential water-quality degradation due to excessive sedimentation.

Figure 9 shows percent of total incremental flux generated for (a) agricultural lands, (b) developing lands, (c) forested lands, and (d) stream channels, suggesting the relative contributions from the various source at each sub-basin. The contributions from these sources that go into the sub-basin yield (Fig. 8) are assessed by comparing predicted sub-basin yield with predicted yield from agricultural-land sediment yield (Fig. 9 (a)); predicted developing-land sediment yield (Fig. 9(b)); predicted forest-land sediment yield (Fig. 9 (c)); and predicted steam channels yield (Fig. 9(d)). Generally, the spatial distribution of these contributions from different sources is in accordance with land use (Fig. 4). On average we can see that 35.11% of incremental flux is from agricultural lands, which is the largest of all sources; the second largest is from forested lands, the value of which is around 23.42%, followed by developing lands (22.91%); the least is from stream channels with a value of 18.56%.

Formatted: Highlight

Formatted: Highlight

Formatted: Highlight

Formatted: Highlight

3.3 Uncertainty analysis

Uncertainty always exists in hydrological models such as SPARROW and therefore cannot imperfect reflect of reality. The sources of uncertainty in this study include: -1) resolution of the geospatial data; 2) quality of the sediment loads used to calibrate the model; and 3) limitations of

the modeling approach in representing the environmental processes accurately (Alexander et al., 2007). First, the hydrologic network was derived from a 50 m digital elevation model (DEM), which potentially deviates from the actual stream network, causing the discrepancy of stream reach and sub-basin characteristics such as stream length, local and total drainage area. This will lead to spatial uncertainty, although that uncertainty is generally reflected in the SPARROW model errors after the calibration process (Alexander et al., 2007). Another cause of uncertainty is suitability of using SS grab samples at the 31 monitoring sites for model calibration to reflect the normal conditions in-stream. Also, the SS loads at some monitoring stations were estimated using the MOVE.3 and LOADEST techniques (Runkel et al., 2004; Duan et al., 2013), which also have some uncertainties.

4 Conclusions

In this study, we developed a SPARROW-based sediment model for surface waters in the Ishikari River basin, the largest watershed in Hokkaido, Japan. This model is based on stream water-quality monitoring records collected at 31 stations for the period 1985 to 2010 and uses four source variables including developing lands, forest lands, agricultural lands, and stream channels, three landscape delivery variables including slope, soil permeability, and precipitation, two in-stream loss coefficients including small stream (drainage area $\leq 200 \text{ km}^2$) and big stream (drainage area $> 200 \text{ km}^2$), and reservoir attenuation. Significant conclusions of the calibration procedure and model application are summarized below. Calibration results explain approximately 95.96% of the spatial variation in the natural logarithm of mean annual SS flux ($\text{kg km}^{-2}\text{yr}^{-1}$) and display relatively small prediction errors on the basis of 31 monitoring stations. Developing-land is associated with the largest intrinsic sediment yield at around $1006.27 \text{ kg km}^{-2}\text{yr}^{-1}$, followed by agricultural-land ($234.21 \text{ kg km}^{-2}\text{yr}^{-1}$). Greater basin slope, less permeable soils, and greater rainfall can directly and indirectly enable sediment transport from land into streams. Reservoir attenuation (26.28 m yr^{-1}) is statistically significant, suggesting that reservoirs can play a dramatic role in

Comment [MM7]: I agree that the computed value is given with many digits, but this precision of the results is not true – please, give only significant digits when presenting results. Especially if in front of this you quote “at around”, and then you give two decimal digits.

Formatted: Highlight

Formatted: Highlight

405 sediment interception. The percent of total incremental flux generated for agricultural lands,
406 developing lands, forested lands, and stream channels is 35.11%, 23.42%, 22.91% and 18.56%,
407 respectively. Sediment total yields and incremental yields concentrate in the sub-basin along the
408 middle and lower reaches of the Ishikari River, showing which sub-basin is most susceptible to
409 erosion. Combined with land use, management actions should be designed to reduce sedimentation
410 of agricultural lands and developing lands in the sub-basin along the middle and lower reaches of
411 the Ishikari River. Our results suggest several areas for further research, including explicit
412 representation of flow and sediment discharge from each stream and in total to the Sea of Japan,
413 more accurate representation of spatial data in SPARROW, and the design of pollutant reduction
414 strategies for local watersheds.

Formatted: Highlight

415 This study also have a number of shortcomings and suggests several areas for future work.
416 Some important model parameters lack statistical significance. For example, statistically
417 insignificant model components and inaccuracies associated with river system, which contain a
418 source variable (stream channels), and big streams with drainage area $>200 \text{ km}^2$. These findings are
419 contrary to the findings of other researches (Brakebill et al., 2010). In addition, the predictions of
420 the model pertain to mean-annual conditions, not necessarily critical conditions such as low- flow
421 conditions. The reason for these shortcomings derives from the following points: (1) the hydrologic
422 network was derived from a 50 m digital elevation model (DEM), which potentially deviates from
423 the actual stream network; (2) due to lack of water discharge in all streams, stream velocity was
424 replaced with drainage area to classify fast and slow streams; and (3) the calibration data only
425 incorporate monitored-load data from limited number of stations with long-term data.

Formatted: Font: 12 pt

Formatted: Font: 12 pt

426 Excessive sedimentation can have a variety of adverse effects on aquatic ecosystems and
427 water resources infrastructure. Analysis of sediment production and transport mechanisms is
428 therefore necessary to describe and evaluate a basin's water quality conditions in order to provide
429 guidance for development of water quality indicators and pollution prevention measures (Buggy

430 and Tobin, 2008; Meals et al., 2010). As illustrated here, the SPARROW model is a valuable tool
431 that can be used by water-resources managers in water-quality assessment and management
432 activities to support regional management of sediment in large rivers and estuaries.

433 Acknowledgements

434 This study is sponsored by the Kyoto University Global COE program
435 “Sustainability/Survivability Science for a Resilient Society Adaptable to Extreme Weather
436 Conditions” and “Global Center for Education and Research on Human Security Engineering for
437 Asian Megacities”, the Postdoctoral fellowship of Japan Society for the Promotion of Science
438 (P12055), JSPS KAKENHI Grant Number 24-02055 and the JSPS Grant-in-Aid for Young
439 Scientists (B) (KAKENHI Wakate B, 90569724). We also wish to acknowledge Anne B. Hoos and
440 John W. Brakebill of the U.S. Geological Survey for their help with the use of SPARROW model.
441 The first author would like to thank China Scholarship Council (CSC) for his PhD scholarships.

442

443 References

- 444 Ahn, Y.S., Nakamura, F., Kizuka, T. and Nakamura, Y., 2009. Elevated sedimentation in lake
445 records linked to agricultural activities in the Ishikari River floodplain, northern Japan. *Earth*
446 *Surf. Proc. Land*, 34(12): 1650-1660.
- 447 Alexander, R.B. et al., 2007. Differences in phosphorus and nitrogen delivery to the Gulf of Mexico
448 from the Mississippi River Basin. *Environ. Sci. Technol.*, 42(3): 822-830.
- 449 Alexander, R.B., Elliott, A.H., Shankar, U. and McBride, G.B., 2002. Estimating the sources and
450 transport of nutrients in the Waikato River Basin, New Zealand. *Water Resour. Res.*, 38(12):
451 1268.
- 452 Alexander, R.B., Smith, R.A. and Schwarz, G.E., 2000. Effect of stream channel size on the
453 delivery of nitrogen to the Gulf of Mexico. *Nature*, 403(6771): 758-761.
- 454 Asahi, K., Kato, K. and Shimizu, Y., 2003. Estimation of Sediment Discharge Taking into Account
455 Tributaries to the Ishikari River. *Journal of natural disaster science*, 25(1): 17-22.
- 456 Asselman, N.E.M., Middelkoop, H. and Van Dijk, P.M., 2003. The impact of changes in climate
457 and land use on soil erosion, transport and deposition of suspended sediment in the River Rhine.
458 *Hydrol. Process*, 17(16): 3225-3244.

Formatted: Highlight

Formatted: Highlight

Formatted: Highlight

Comment [MM8]: This reference is not used in the text.

Formatted: Highlight

Formatted: Highlight

Formatted: Highlight

Formatted: Highlight

Formatted: Highlight

- 459 Bilotta, G.S. and Brazier, R.E., 2008. Understanding the influence of suspended solids on water
460 quality and aquatic biota. *Water Res.*, 42(12): 2849-2861. Formatted: Highlight
- 461 Brakebill, J.W., Ator, S.W. and Schwarz, G.E., 2010. Sources of Suspended - Sediment Flux in
462 Streams of the Chesapeake Bay Watershed: A Regional Application of the SPARROW Model1.
463 JAWRA *Journal of the American Water Resources Association*, 46(4): 757-776. Formatted: Highlight
- 464 Buggy, C.J. and Tobin, J.M., 2008. Seasonal and spatial distribution of metals in surface sediment
465 of an urban estuary. *Environ. Pollut.*, 155(2): 308-319. Formatted: Highlight
- 466 Chapra, S. C., 1997. *Surface Water-Quality Modelling*, McGraw-Hill, New York. Formatted: Highlight
- 467 Conley, D.J. et al., 2009. Controlling eutrophication: nitrogen and phosphorus. *Science*, 323(5917):
468 1014-1015.
- 469 Dedkov, A.P. and Mozzherin, V.I., 1992. Erosion and sediment yield in mountain regions of the
470 world. *Erosion, debris flows and environment in mountain regions*, 209: 29-36. Formatted: Highlight
- 471 Drewry, J.J., Newham, L. and Croke, B., 2009. Suspended sediment, nitrogen and phosphorus
472 concentrations and exports during storm-events to the Tuross estuary, Australia. *J Environ.*
473 *Manage.*, 90(2): 879-887. Formatted: Highlight
- 474 Duan, W. et al., 2013. Spatial and temporal trends in estimates of nutrient and suspended sediment
475 loads in the Ishikari River, Japan, 1985 to 2010. *Sci. Total Environ.*, 461: 499-508. Formatted: Highlight
Formatted: Highlight
- 476 Fang, N.F., Shi, Z.H., Li, L. and Jiang, C., 2011. Rainfall, runoff, and suspended sediment delivery
477 relationships in a small agricultural watershed of the Three Gorges area, China. Formatted: Highlight
478 *Geomorphology*, 135(1-2): 158-166.
- 479 FAO-UNESCO-ISRIC, 1988. FAO-UNESCO soil map of the world: revised legend. FAO Rome,
480 Italy. Formatted: Highlight
- 481 Hoos, A.B. and McMahon, G., 2009. Spatial analysis of instream nitrogen loads and factors
482 controlling nitrogen delivery to streams in the southeastern United States using spatially
483 referenced regression on watershed attributes (SPARROW) and regional classification
484 frameworks. *Hydrol Process*, 23(16): 2275-2294. Formatted: Highlight
- 485 Hunter, H.M. and Walton, R.S., 2008. Land-use effects on fluxes of suspended sediment, nitrogen
486 and phosphorus from a river catchment of the Great Barrier Reef, Australia. *J. Hydrol.*, 356(1):
487 131-146. Formatted: Highlight
- 488 Ishida, T. et al., 2010. Suspended sediment transport in a river basin estimated by chemical
489 composition analysis. *Hydrological Research Letters*, 4(0): 55-59. Formatted: Highlight
Formatted: Highlight
Formatted: Highlight
- 490 Julien, P.Y. and Simons, D.B., 1985. Sediment transport capacity of overland flow. *Trans. ASAE*,
491 28(3): 755-762. Formatted: Highlight
- 492 Lal, R., 2001. Soil degradation by erosion. *Land Degrad Dev*, 12(6): 519-539. Formatted: Highlight

493 | Langland, M.J. and Cronin, T.M., 2003. A summary report of sediment processes in Chesapeake
494 | Bay and watershed. U.S. Geological Survey. XXXXXXXX

495 | Le, C. et al., 2010. Eutrophication of lake waters in China: cost, causes, and control. Environ.
496 | Manage, 45(4): 662-668.

497 | Luce, C.H. and Black, T.A., 1999. Sediment production from forest roads in western Oregon. Water
498 | Resour. Res., 35(8): 2561-2570.

499 | McMahon, G., Alexander, R.B. and Qian, S., 2003. Support of total maximum daily load programs
500 | using spatially referenced regression models. Journal of Water Resources Planning and
501 | Management, 129(4): 315-329.

502 | Meade, R.H., Dunne, T., Richey, J.E., DeE M Santos, U. and Salati, E., 1985. Storage and
503 | remobilization of suspended sediment in the lower Amazon River of Brazil. Science,
504 | 228(4698): 488.

505 | Meals, D.W., Dressing, S.A. and Davenport, T.E., 2010. Lag time in water quality response to best
506 | management practices: A review. J. Environ. Qual., 39(1): 85-96.

507 | Mizugaki, S. et al., 2008. Estimation of suspended sediment sources using 137Cs and 210Pbex in
508 | unmanaged Japanese cypress plantation watersheds in southern Japan. Hydrol. Process., 22(23):
509 | 4519-4531.

510 | Nearing, M.A. et al., 2005. Modeling response of soil erosion and runoff to changes in precipitation
511 | and cover. Catena, 61(2): 131-154.

512 | Nelson, E.J. and Booth, D.B., 2002. Sediment sources in an urbanizing, mixed land-use watershed.
513 | J. Hydrol., 264(1): 51-68.

514 | Preston, S. D., Alexander, R. B., Woodside, M. D., and Hamilton, P. A., 2009. SPARROW
515 | modeling: Enhancing understanding of the nation's water quality. USGS Fact Sheet 2009-3019.
516 | USGS, Reston, VA.

517 | Ran, Q., Su, D., Li, P. and He, Z., 2012. Experimental study of the impact of rainfall characteristics
518 | on runoff generation and soil erosion. J. Hydrol., 424: 99-111.

519 | Ruddy, B. C., D. L. Lorenz, and D. K. Mueller (2006), County-level estimates of nutrient inputs to
520 | the land surface of the conterminous United States, 1982–2001, U.S. Geol. Surv. Sci. Invest.
521 | Rep., 2006–5012, 17 pp.

522 | Runkel, R.L., Crawford, C.G., Cohn, T.A., 2004. Load Estimator (LOADEST): A FORTRAN
523 | Program for Estimating Constituent Loads in Streams and Rivers. U. S. Geological Survey, p.
524 | 69.

525 | Schwarz, G.E., 2008. A Preliminary SPARROW Model of Suspended Sediment for the
526 | Conterminous United States. U.S. Geological Survey Open-File Report 2008-1205. U.S.

Geological Survey, Reston, VA. <http://pubs.usgs.gov/of/2008/1205> (accessed 2013.04.09).

Schwartz, G. E., Hoos, A. B., Alexander, R. B., Smith, R. A., 2006. The SPARROW surface water-quality model: Theory, application, and user documentation; U.S. Geological Survey Techniques and Methods Report; Vol. 6, Chapter B3.

Smith, R.A., Schwarz, G.E. and Alexander, R.B., 1997. Regional interpretation of water-quality monitoring data. *Water Resour. Res.*, 33(12): 2781-2798.

Somura, H., Takeda, I., Arnold, J. G., Mori, Y., Jeong, J., et al., 2012. Impact of suspended sediment and nutrient loading from land uses against water quality in the Hii River basin, Japan. *J. Hydrol.* 450: 25-35.

Srinivasa, G., S., Ramakrishna, R., M. and Govil, P.K., 2010. Assessment of heavy metal contamination in soils at Jajmau (Kanpur) and Unnao industrial areas of the Ganga Plain, Uttar Pradesh, India. *J Hazard Mater.*, 174(1): 113-121.

Trimble, S.W., 1997. Contribution of stream channel erosion to sediment yield from an urbanizing watershed. *Science*, 278(5342): 1442-1444.

U.S. Environmental Protection Agency USEPA, 2006. Wadeable streams assessment: a collaborative survey of the nation's streams.

Vogel, R.M. and Stedinger, J.R., 1985. Minimum variance streamflow record augmentation procedures. *Water Resour. Res.*, 21(5): 715-723.

Wolman, M.G., 1967. A cycle of sedimentation and erosion in urban river channels. *Geografiska Annaler. Series A. Physical Geography*: 385-395.

Wongsa, S. and Shimizu, Y., 2004. Modelling artificial channel and land - use changes and their impact on floods and sediment yield to the Ishikari basin. *Hydrol. Process.*, 18(10): 1837-1852.

Formatted: German (Germany)

Formatted: German (Germany), Highlight

Formatted: German (Germany)

Formatted: Highlight

Formatted: Highlight

Formatted: Highlight

Formatted: Highlight

Formatted: Highlight

Formatted: Highlight

Formatted: Highlight

Formatted: Highlight

Formatted: Highlight

550 **Table 1.** Summary of input data and calibration parameters. References to data sources are in the
551 main text

Category	Input data	Data source
The stream network	Stream network, stream lengths, sub-catchment boundaries, sub-catchment areas	Automated catchment delineation based on a 50 m DEM, with modification of flow diversions
Stream load data	Water quality monitoring station	Thirty one stations from the National Land with Water Information monitoring network from 1982 to 2010
Sediment source data	Developing land, forest land, and agricultural land	Land use data including developing land, forest land, agricultural land from the Ministry of Land, Infrastructure, Transport and Tourism, Japan, 2006
Environmental setting data	Mean annual precipitation	The 20-year (1990-2010) average from Japanese Meteorological Agency
	Catchment slope	Mean value of local slope, obtained from 50 m DEM
	Soil texture, soil permeability	Obtained from the 1:5.000.000-scale FAO/UNESCO Soil Map of the World and the National and Regional Planning Bureau, Japan
	Reservoir (dams) loss	The Japan Dam Foundation (http://damnet.or.jp/)

554

Table 2. SPARROW estimates of model statistics for Ishikari River basin SS

Model parameters	Coefficient units	Estimated coefficient	Standard error	P-value
SS sources				
Developing land	kg km ⁻² yr ⁻¹	1006.267	508.503	0.028
Forest land	kg km ⁻² yr ⁻¹	75.554	31.058	0.011
Agricultural land	kg km ⁻² yr ⁻¹	234.211	121.7511	0.036
Streambed (stream channels)	kg km ⁻² yr ⁻¹	123.327	99.567	0.113
Land-to-water loss coefficient				
Slope	-	0.349	0.094	<0.001
Soil permeability	hr cm ⁻¹	-9.195	2.431	<0.001
Precipitation	mm	0.007	0.002	<0.002
In-stream loss rate				
Small stream (drainage area ≤200 km ²)	day ⁻¹	-0.044	0.011	<0.001
Big stream (drainage area >200 km ²)	day ⁻¹	0.000012	0.0068	>0.050
Reservoir-loss	m yr ⁻¹	26.283	4.364	<0.001
Model diagnostics				
Mean square error	0.323			
Number of observations	31			
R-squared	0.9596			

555

556

557

558

559

560

561

562

563

564

Notes: SPARROW, SPATIally Referenced Regression on Watershed; kg, kilograms; km, kilometers; yr, year; >, more than; <, less than. This table shows overall model calibration results, statistical parameter estimates, standard errors, and probability levels for modeled explanatory variables representing sediment sources, landscape factors affecting the delivery of sediment from uplands to streams (land-to-water), and in-stream and reservoir storage. All sources and storage terms are constrained to nonnegative estimates for more physically realistic simulations of sediment transport. Because of this specification, statistical significance for source and aquatic storage coefficient estimates are reported as a one-sided p statistic. Probability levels for land-to-water parameters are two-sided values (Schwarz et al., 2006).

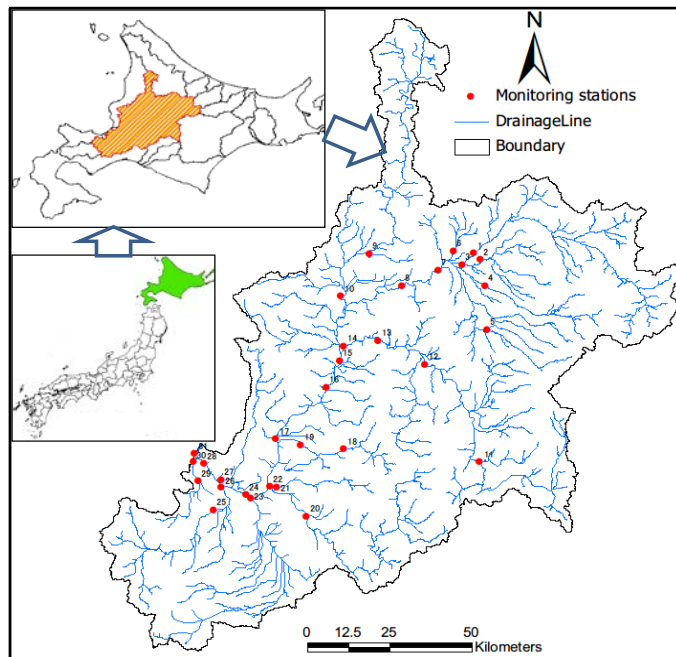


Figure 1. Study area, stream networks, and monitoring stations for the Ishikari River basin

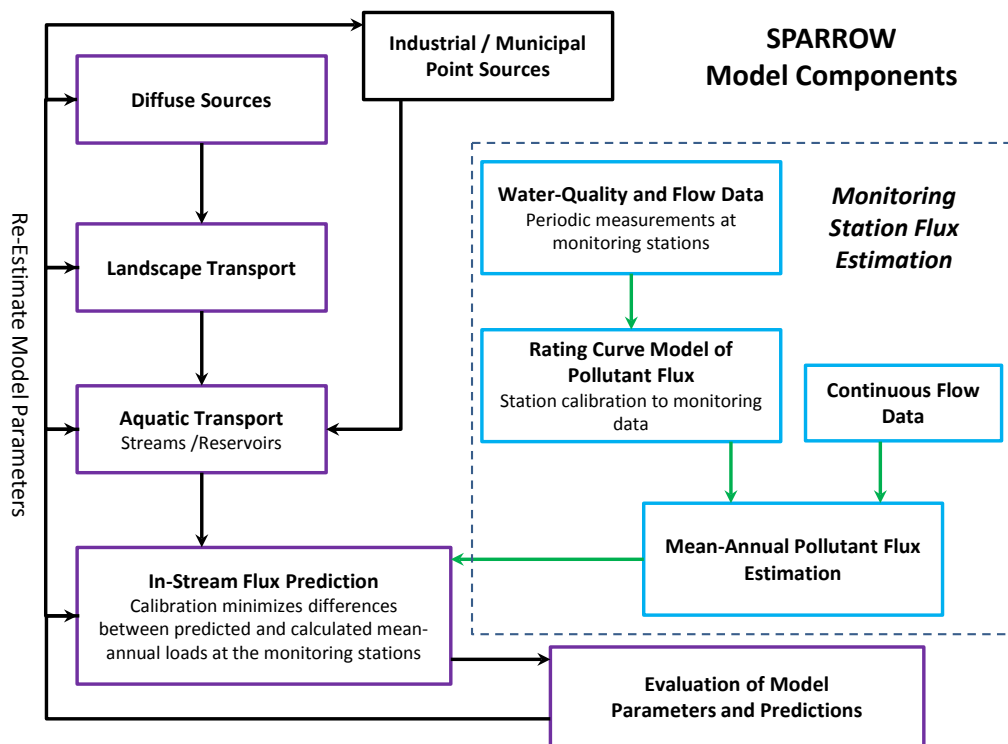


Figure 2. Schematic of the major SPARROW model components (from Schwarz et al., 2006)

571
572
573
574

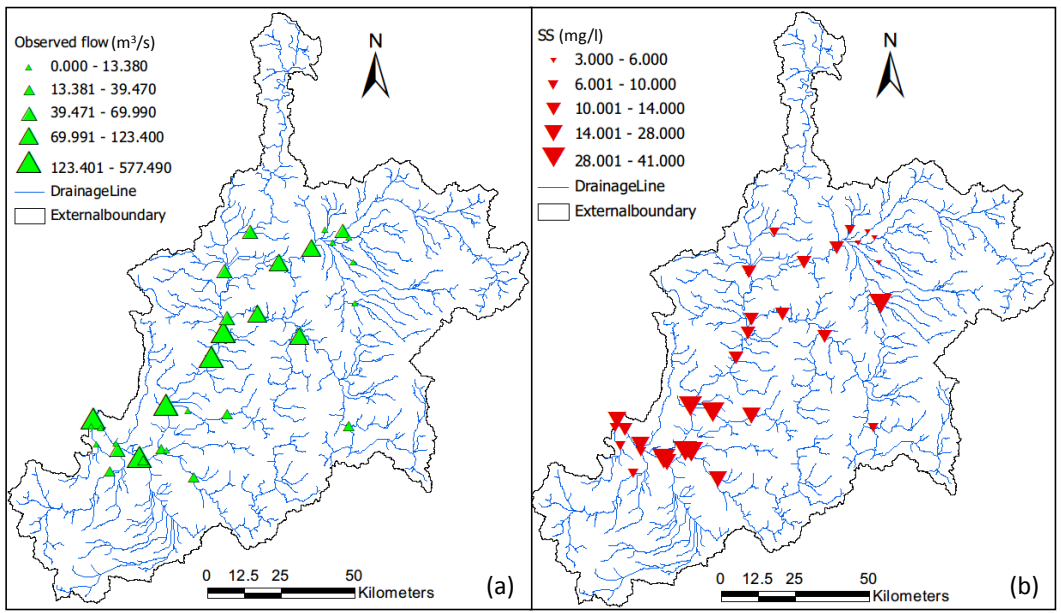


Figure 3. Schematic showing (a) the observed water flows (m^3/s) and (b) the observed SS concentration (mg/l) at 31 monitoring stations

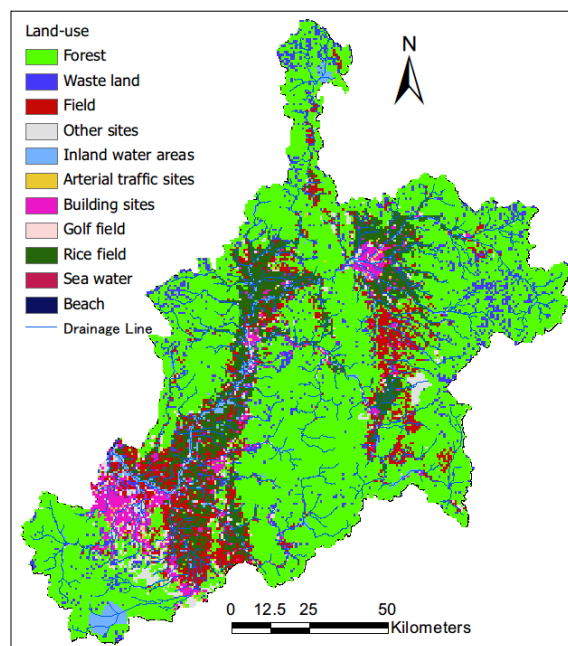


Figure 4. Land use of the Ishikari River basin, 2006

578
579
580

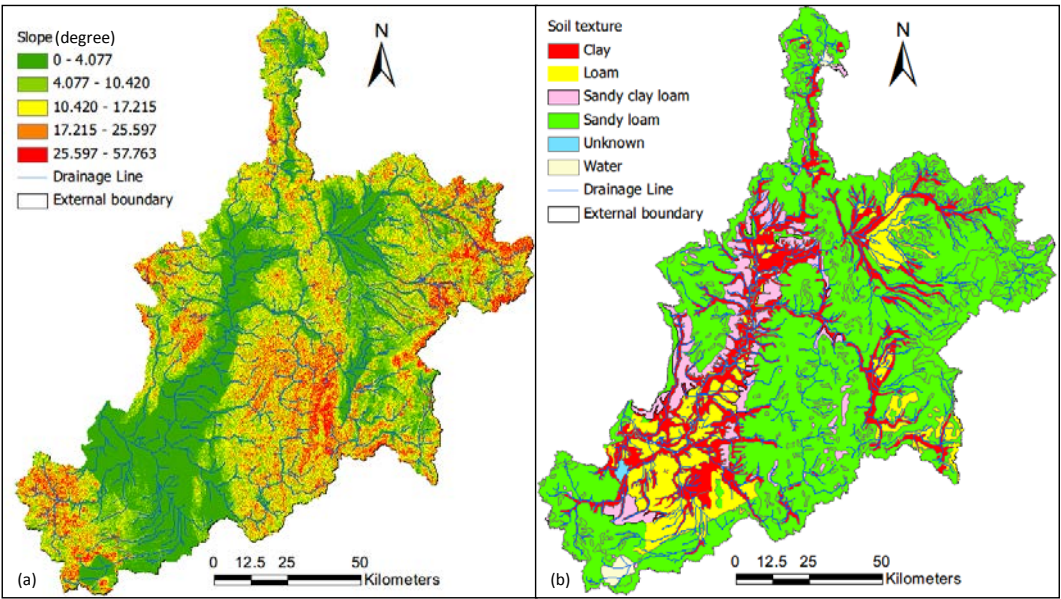


Figure 5. Schematic showing the slope (a) and soil texture (b) in Ishikari river basin

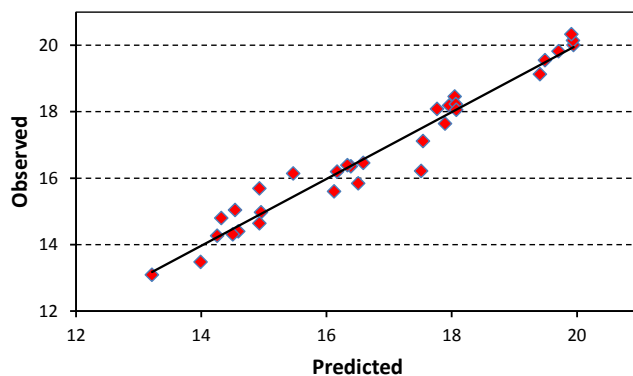


Figure 6. Observed and predicted SS flux (kg/yr) at 31 monitoring sites included in the Ishikari SPARROW model
(Natural logarithm transformation applied to observed and predicted values)

Comment [MM9]: You may present this figure in a quadratic form. You are showing observed and predicted values and the slope should be 1:1 at 45 degrees.

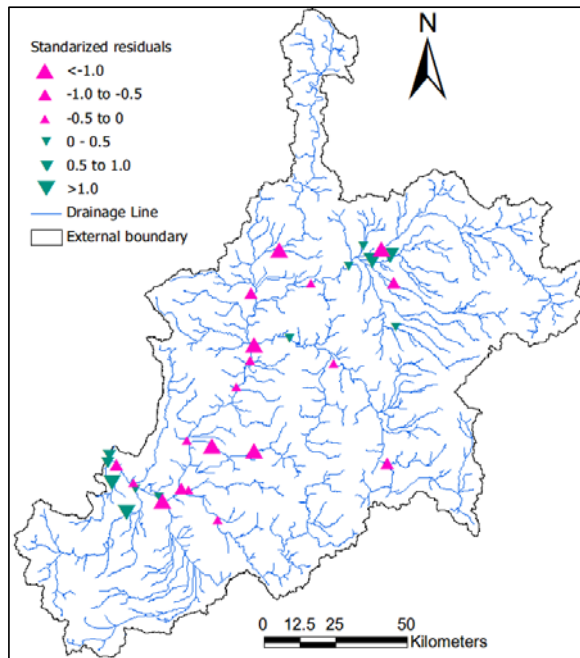


Figure 7. Model residuals for 31 monitoring stations used to calibrate the final Ishikari SPARROW model

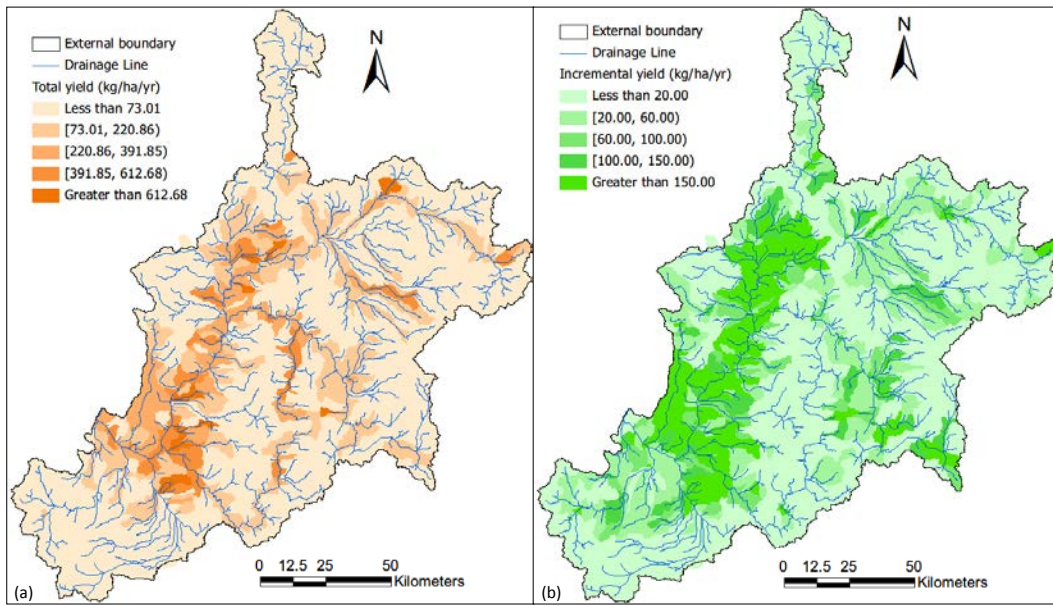


Figure 8. Map showing the spatial distribution of total suspended sediment yields (a) and incremental suspended sediment yields (b) estimated by SPARROW.

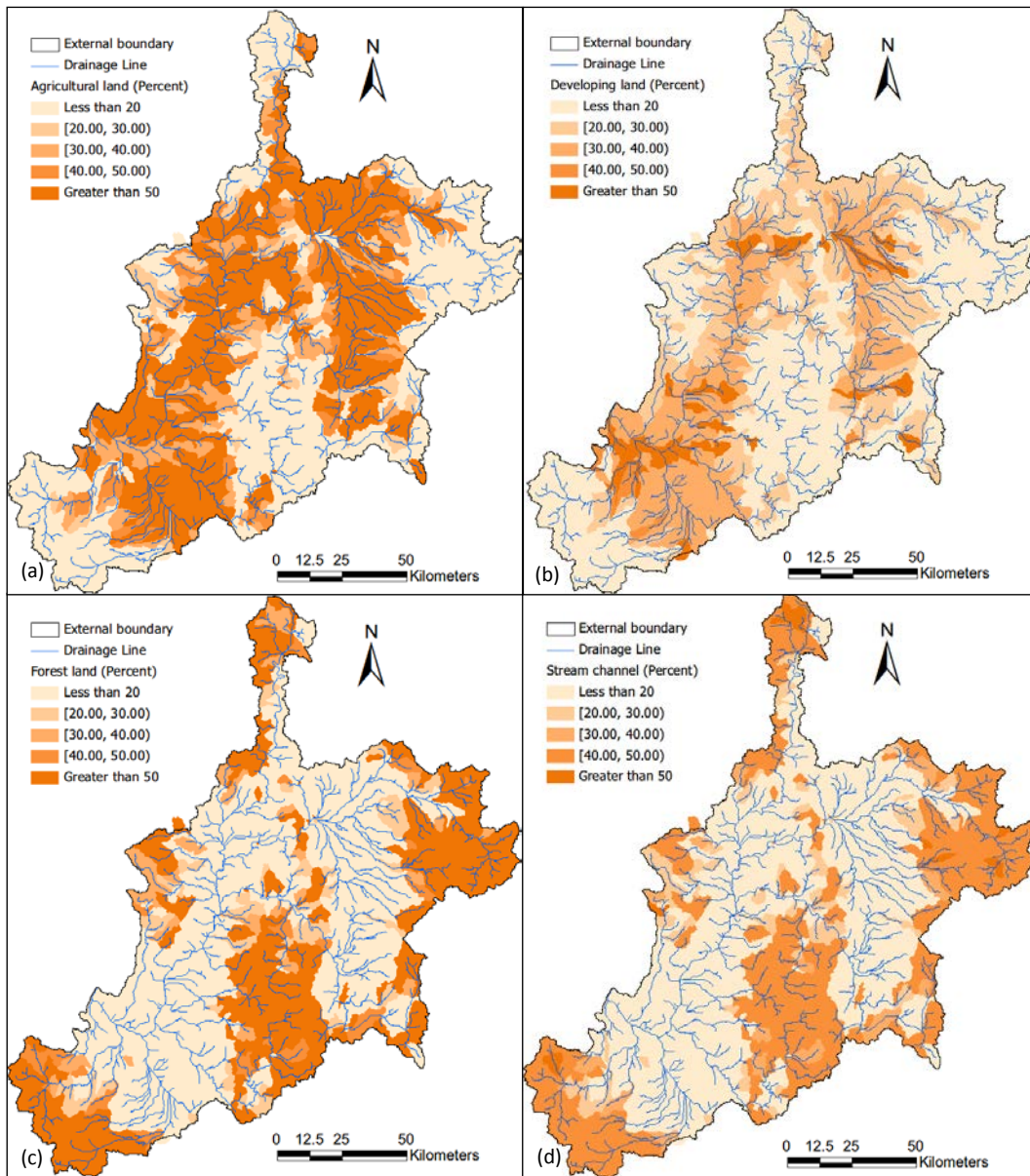


Figure 9. Maps showing the spatial distributions of independent sediment sources generated in each incremental catchment for (a) agricultural land, (b) developing land, (c) forested land, and (d) stream channel.